Available online at www.sciencedirect.com
ScienceDirect
Trans. Nonferrous Met. Soc. China 25(2015) 1692−1698
Transactions of Nonferrous Metals Society of China
www.tnmsc.cn

Electrochemical behavior of Pb−Ag−Nd alloy during pulse current polarization in H_2SO_4 solution

Xiao-cong ZHONG[1], Xiao-ying YU[1], Liang-xing JIANG[1], Fei LI[2], Jie LI[1], Ye-xiang LIU[1]

1. School of Metallurgy and Environment, Central South University, Changsha 410083, China;
2. Henan Yuguang Zinc Industry Co. Ltd., Jiyuan 459000, China

Received 17 June 2014; accepted 9 September 2014

Abstract: The anodic layer and oxygen evolution behavior of Pb−Ag−Nd alloy during pulse current polarization and constant current polarization in 160 g/L H_2SO_4 solution was comparatively investigated by chronopotentiometry, SEM, XRD, EIS and Tafel techniques. The results show that the anodic layer on Pb−Ag−Nd alloy formed through pulse current polarization is more intact and presents fewer micro-holes than that formed through constant current polarization. This could be attributed to the low current density period, which works as a 'recovery period'. During this period, the oxygen evolution reaction is less intense, which benefits the recovery of porous anodic layer. Pb−Ag−Nd anode also shows a lower anodic potential during pulse current polarization, which is in accordance with its smaller charge transfer resistance and smaller Tafel slope coefficient at high over-potential region. The lower anodic potential could be ascribed to the higher concentration of PbO_2 in the anodic layer, which promotes the formation of more reactive sites for the oxygen evolution reaction.

Key words: Pb-based anode; pulse current polarization; oxygen evolution behavior; anodic layer

1 Introduction

Pb-based anodes have been widely used in hydrometallurgical electrowinning of Zn, Cu, Ni, Co and Mn [1−4]. Most research publications on Pb-based anodes are based on constant current polarization. Actually, in industrial practice, the current passing the anodes is not constant. Taking Zn electrowinning as example, during the Zn stripping operation, the anodic current would descend to a lower level. In addition, due to the multi-step electricity pricing policy, hydrometallurgical plants tend to apply low current density during the peak electricity periods and high current density during the off-peak electricity periods, because this current pattern is beneficial to decreasing the electricity cost and ensuring the product output simultaneously. Hence, the anodes are under pulse current anodization rather than constant current anodization in industrial practice.

It is well known that pulse current techniques have shown many advantages compared with the direct current (DC) techniques, such as pulse current electrodeposition, which facilitates to obtain controllable particle size, strong adhesion, uniform electrodeposition and small internal stress [5,6]. Similarly, pulse current anodization can be applied to fabricate structurally well defined material as well, like Ni−P coatings [7], Ni−W−P/CeO_2−SiO_2 composites [8] and Al/Pb−PANI−WC inert anode [9]. However, limited publications have reported the electrochemical behavior of Pb-based anodes during pulse-current polarization [10,11]. TAGUCHI et al [10] reported the effect of Sr on the corrosion behavior of Pb−Sn alloy during the repetitive current application. MASSÉ and PIRON [11] investigated the anodic potential current response and the cathodic current efficiency during Zn electrowinning using periodical reverse current (PRC), and the result showed that PRC could decrease the energy consumption and improve the morphology of anode. However, these studies did not reveal the influence of pulse current on the corrosion behavior and oxygen evolution behavior of Pb-based anode systematically. The correlation between the properties of the anodic layer, the oxygen evolution

Foundation item: Projects (51204208, 51374240) supported by the National Natural Science Foundation of China; Project (2012BAA03B04) supported by the National Science and Technology Pillar Program of China; Project (2014zzts028) supported by the Fundamental Research Funds for the Central Universities of Central South University, China

Corresponding author: Liang-xing JIANG; Tel: +86-731-88830474; E-mail: lxjiang@csu.edu.cn

DOI: 10.1016/S1003-6326(15)63774-8

kinetics with the current pattern remains unclear.

In this work, the anodic behaviors of Pb−Ag−Nd alloy in H_2SO_4 solution during pulse current polarization and constant current polarization were investigated comparatively. The influence of pulse-current polarization on the anodic potential, morphology and phase composition of the anodic layer and the oxygen evolution kinetics was investigated separately. With improved understanding of the anodic behavior of Pb-based anode during pulse current polarization, it is practical to evaluate the influence of pulse current pattern on the performance of Pb-based anodes. Furthermore, the hydrometallurgical plants could adjust the current pattern to decrease the electricity consumption and to improve the performance of Pb-based anodes.

2 Experimental

The Pb−0.45Ag−0.03Nd (mass fraction, %) alloy was cut into cuboid anodes (10 mm × 10 mm × 7 mm). These anodes were sealed by the denture base resin with an exposed geometric area of 1.0 cm^2. All the electrochemical measurements were carried out with a three-electrode system in 160 g/L H_2SO_4 solution. The working electrodes were ground with SiC sand paper gradually from 360 grit to 2000 grit before each electrochemical measurement. A Pt plate (4 cm^2) and Hg/Hg_2SO_4/saturated K_2SO_4 (0.64 V vs standard hydrogen electrode) were used as the counter electrode and reference electrode, respectively. All potentials in this work are referred to the reference electrode. Each electrochemical measurement was conducted on an electrochemical workstation (1470 E, Solartron Analytical, UK) at (35±0.5) °C.

Both constant current and pulse current were used in this work, as shown in Fig. 1. The total polarization time is 80 h for both current patterns. As for the pulse-current polarization, two current densities, namely J_H (500 A/m^2) and J_L (350 A/m^2), were applied according to the industrial operation condition. In Fig. 1, T is one pulse period, and its value is 24 h. t_H and t_L refer to the duration time of high and low current density in one pulse period, and their values are 20 h and 4 h, respectively.

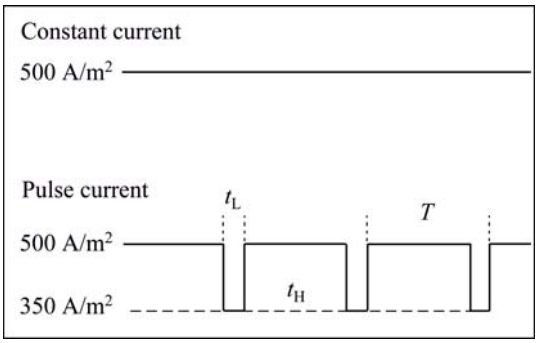

Fig. 1 Two current patterns used for polarization of Pb−Ag−Nd anode

During the 80 h polarization, the anodic potential was recorded by the electrochemical workstation. After the polarization, the anodic layers obtained were analyzed with scanning electron microscopy (MIRA 3, TESCAN, Czech Republic) and X-ray diffractometer (D/max 2500, Rigaku Co., Japan).

In addition, after the 80 h polarization, electrochemical impedance spectroscopy and Tafel measurements were carried out separately. During the impedance measurements, the amplitude of AC signal was 10 mV, and the frequency ranged from 100 kHz to 0.1 Hz. The DC bias potentials measured at the end of the 80 h polarization were set as the anodic potential. The Tafel tests were carried out with the potential ranging from 1.52 to 1.22 V, and the scanning rate was 0.166 mV/s.

3 Results and discussion

3.1 Anodic potential variation

Figure 2 depicts the potential variation of Pb−Ag−Nd anode during the constant current and pulse current polarization. At the beginning of the constant current polarization, the anodic potential descends rapidly because of the low over-potential for the oxidation of Pb to $PbSO_4$. With the coverage of high resistance $PbSO_4$ on the anode increases, the anodic potential shows a slight increase, and peeks at 1.385 V when the polarization time reaches 10 h. Then the anodic potential descends sustainedly due to the transformation of $PbSO_4$ to the conductive PbO_2, which benefits the oxygen evolution reaction (OER) because the PbO_2 facilitates the formation of reactive sites for OER [9,10]. As for the pulse current polarization, the anodic potential

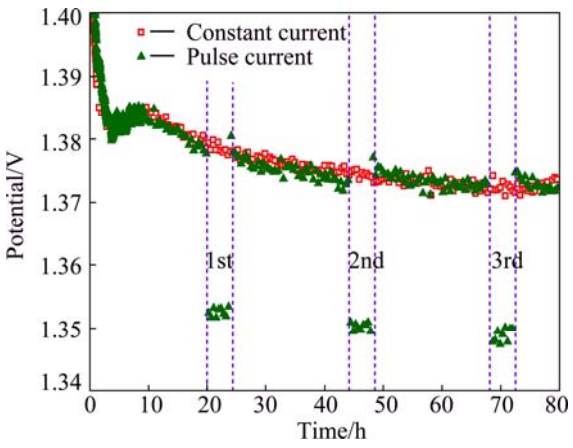

Fig. 2 Anodic potentials of Pb−Ag−Nd anodes during 80 h polarization

shows a descending trend as well. During the low current period, the anodic polarization is much smaller, and the OER is less intense. Hence, the anodic potential is about 1.35 V, which is about 35 mV lower than that during the high current period. At the end of polarization, the anodic potential under the pulse current polarization is slightly lower.

Figure 3 shows the potential variation when the current density steps from 500 to 350 A/m^2 (Fig. 3(a)) and from 350 to 500 A/m^2 (Fig. 3(b)). During the downward and upward pulse, it takes about 500 s for the anodic reaction to reach a steady state, and about 10 min for the anodic potential to reach a stable value. During a downward pulse, the anodic potential drops to a minimum value at the very beginning, then ascends by 10 mV in the first 10 min. Similarly, the anodic potential descends by about 5 mV in the first 10 min during each upward pulse. It is notably that the anodic potential during the 2nd downward pulse is about 3 mV lower than that during the 1st pulse, and the anode shows the lowest stable potential during the 3rd pulse. Similarly, during the upward pulse, the anodic potential during the 3rd pulse is also the lowest. This could be attributed to the concentration of PbO_2 in the anodic layer increases as the polarization continues. In addition, it can be found that the potential variations during both the 3rd downward and upward pulse are less intense than that during the 1st and 2nd pulse. It indicates that after several current pulses, the anodic surface becomes more stable and the anodic process could reach a steady state rapidly. It can be inferred that the influence of current pulse on the anodic behavior may become smaller as the polarization continues.

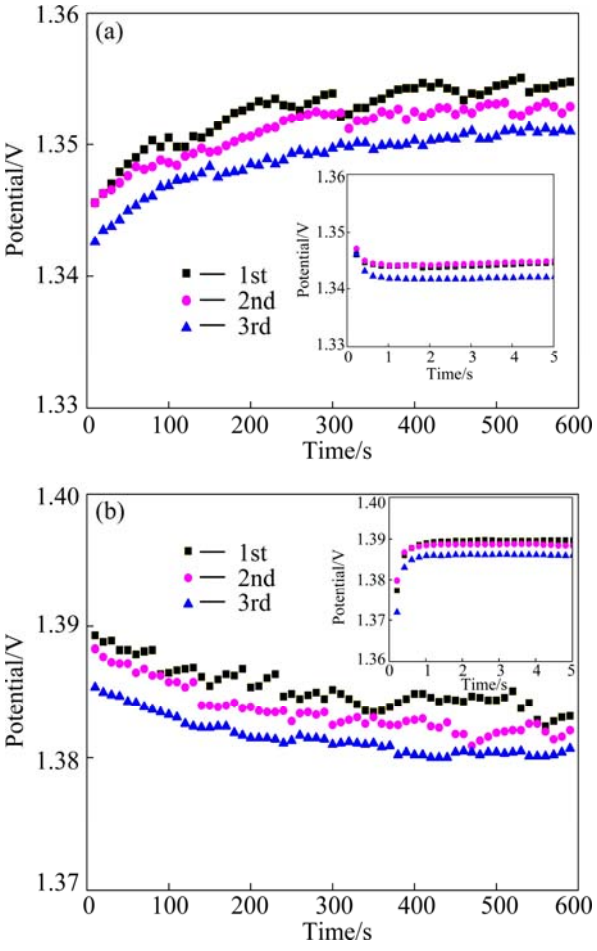

Fig. 3 Anodic potential variation during current steps from 500 to 350 A/m^2 (a) and from 350 to 500 A/m^2 (b)

3.2 Morphology of anodic layer

Figure 4(a) presents the morphology of the anodic layer obtained through 80 h constant current polarization, which features a typical coral-like morphology. The anodic layer is loose, coarse, bearing a large number of micro-holes. This feature could be attributed to the intense impact of oxygen bubbles which accelerate the detaching of Pb compounds, resulting in porous surface of the anodic layer. The micro-holes presented in the anodic layer would facilitate the transfer of electrolyte into the inner part of the anodic layer, resulting in severe corrosion. Additionally, these micro-holes may also further make Pb oxides more readily detach from the anode surface. As for the anodic layer formed through pulse current polarization (Fig. 4(b)), it is more intact than the former one. The number of micro-holes is largely diminished, and the micro-holes are much smaller and shallower. This could be correlated with the

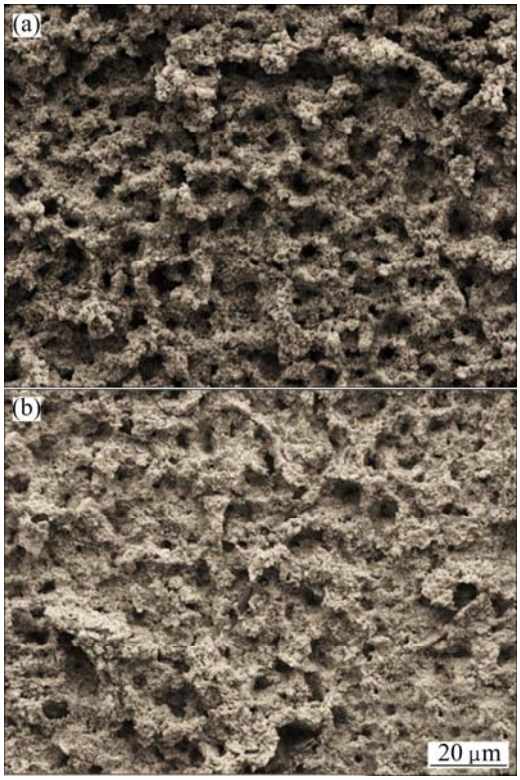

Fig. 4 Morphologies of anodic layers on Pb−Ag−Nd anode obtained through 80 h polarization: (a) Constant current polarization; (b) Pulse current polarization

applied current pattern. During the low current density period, the impact of oxygen bubbles is much less intense, and the anodic film is less readily detached from the anode. Moreover, during the low current density period, the growth of anodic layer at the holes(cracks) existing regions could diminish the number of holes and cracks, benefiting the formation of a more intact and compact anodic layer. Therefore, the low current density period could be regarded as 'recovery period', which improves the quality of the anodic layer. In summary, the pulse current polarization facilitates the formation of mort intact and compact anodic layer, which could provide better protection for the metallic substrates.

3.3 XRD analysis of anodic layer

Figure 5 shows the XRD patterns of the anodic layers obtained through 80 h polarization with constant current and pulse current. It is clear that the anodic layers formed through two current patterns present similar phase composition, with $PbSO_4$ and PbO_2 being the predominant phases. The minority components, such as PbO, non-stoichiometric PbO_n, and Pb basic sulfates are not observed on the XRD patterns due to their limited concentration on the surface of the anodic layers. The intensity of PbO_2 of the anodic layer obtained through pulse current polarization is slightly higher, and the intensity ratio of PbO_2 to $PbSO_4$ for the anodic layer obtained with pulse current is larger. This indicates that the anodic layer obtained with pulse current has higher PbO_2 concentration, which can be explained as follows: the more intact and compact anodic layer facilitates the electric contact between the conductive PbO_2 and the inner part of the anodic layer. Under the anodic polarization, these Pb compounds are less readily dissolved into the electrolyte. Therefore, the concentration of PbO_2 could increase gradually.

3.4 EIS analysis on oxygen evolution behavior

The main reaction on Pb-based anodes during electrowinning is OER. The OER reactivity determines the anodic over-potential, which significantly affects the energy consumption of the electrowinning operation. Therefore, OER reactivity is a critical criterion for the electrochemical performance of Pb-based anodes. The OER kinetics was investigated by EIS and Tafel tests in this work.

EIS technique was adopted widely to investigate OER on metallic oxide electrodes [12−15]. Figure 6 shows the complex planes of Pb−Ag−Nd anodes after 80 h constant current and pulse current polarization. There is only one capacitance arc appearing in the complex planes, indicating that the charge transfer resistance of OER is in parallel with the double layer capacitance [16]. In addition, an obvious inductance, L, is observed at the high frequency region, which can be ascribed to the charge relaxation on electroactive materials containing heterogeneity or energy disorder [17]. The electrical equivalent circuit (EEC) embedded in Fig. 6 was adopted to fit the EIS data. The use of constant phase element (CPE) is a good approach for the study of the solid electrodes with different degrees of surface roughness, physical nonuniformity or a non-uniform distribution of the surface reaction sites [18,19]. Hence, CPE, instead of capacitors (C), was used to fit the experimental data of double layer capacitance (C_{dl}). The impedance of the CPE could be written as [19]

$$Z_{CPE} = \frac{1}{Q(j\omega)^n} \quad (1)$$

where Q is the capacity parameter in $F \cdot cm^{-2} \cdot s^{n-1}$, ω is the angular frequency (s^{-1}), and n represents the deviation from the ideal behavior (n is 1 for the perfect capacitor). BRUG et al [19] proposed that the C_{dl} was coupled with

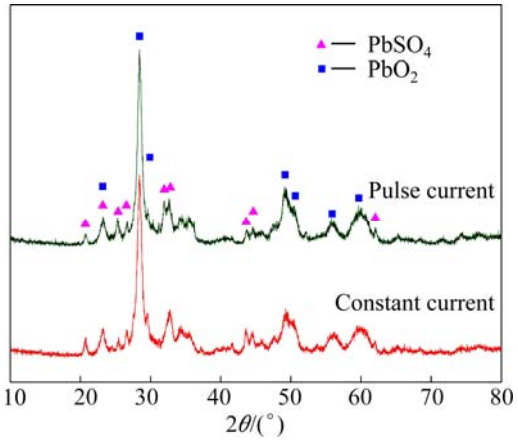

Fig. 5 XRD patterns of anodic layers on Pb−Ag−Nd anode obtained through 80 h polarization with constant current and pulse current

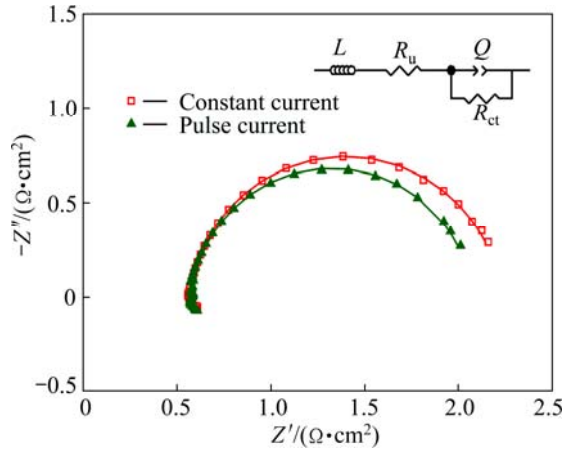

Fig. 6 Nyquist plots of Pb−Ag−Nd anodes after 80 h polarization with constant current and pulse current (scatters for experimental data and lines for simulated data)

the uncompensated resistance R_u and the charge transfer resistance R_{ct}, as expressed as

$$Q = (C_{dl})^n[(R_u)^{-1} + (R_{ct})^{-1}]^{(1-n)} \quad (2)$$

Therefore, C_{dl} was calculated using Q obtained from the EEC fitting. The simulated patterns and the parameters obtained through EEC fitting were shown in Fig. 6 (lines) and Table 1, respectively.

Table 1 Main parameters for EIS data obtained through fitting with EEC embedded in Fig. 6

Current pattern	Constant current	Pulse current
$L/(10^{-7}\ \mathrm{H\cdot cm^2})$	0.99	1.30
$C_{dl}/(10^{-2}\ \mathrm{F\cdot cm^{-2}})$	5.56	5.37
$R_u/(\Omega\cdot\mathrm{cm^2})$	0.567	0.577
$R_{ct}/(\Omega\cdot\mathrm{cm^2})$	1.65	1.50
n	0.93	0.94
$\chi^2/10^{-4}$	2.47	3.91

As shown in Table 1, the chi square (χ^2) values of EEC fitting for both anodes are around 10^{-4}, suggesting that a good approximation can be obtained with EEC shown in Fig. 6. The pulse current polarized Pb−Ag−Nd anode presents smaller double layer capacity (C_{dl}) and charge transfer resistance (R_{ct}). C_{dl} could be used to evaluate the roughness of the anodic layer according to the following equation [20].

$$R_F = \frac{C_{dl}}{C^*} \quad (3)$$

where R_F is a roughness factor, C^* represents the reference value for the capacitance, which is about 20 μF/cm^2 for smooth Hg electrodes. The anodic layer formed during pulse current polarization has a smaller C_{dl}, thus it has a smaller R_F, representing that the anodic layer is smoother as demonstrated in Fig. 4. The smaller C_{dl} can also be explained by the fewer holes on the intact anodic layer, which leads to smaller specific surface area of the anodic layer. Consequently, fewer charged species absorb at the anodic layer/electrolyte interface.

The smaller R_{ct} of pulse current polarized Pb−Ag−Nd anode may be related with the higher concentration of PbO_2 existing in the anodic layer, which is proved by the XRD analysis. The higher concentration of PbO_2 may lead to a larger number of reactive sites for OER. Consequently, the pulse current polarized Pb−Ag−Nd anode presents a lower anodic potential.

3.5 Tafel analysis on oxygen evolution behavior

To further understand the kinetics of OER on Pb−Ag−Nd anode, Tafel tests were conducted after 80 h polarizations. The Tafel curves shown in Fig. 7 were obtained by backward potential sweep. All experimental Tafel curves were corrected by removing the ohmic drop as expressed by [21]

$$E_{eff} = E_{appl} - IR_u \quad (4)$$

where E_{eff} is the effective potential and E_{appl} refers to the applied potential of Pb−Ag−Nd anode, IR_u represents the uncompensated ohmic drop of the anodic process.

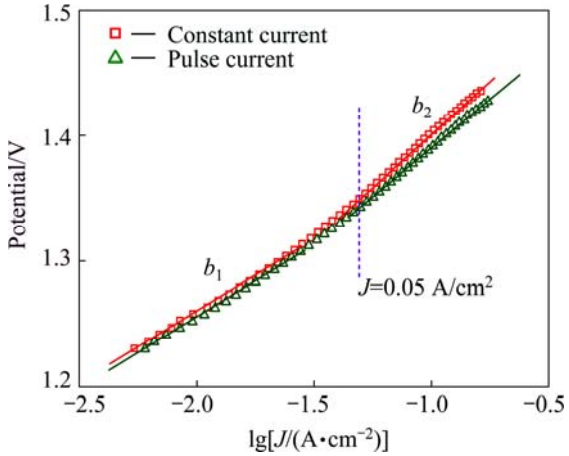

Fig. 7 Tafel curves of Pb−Ag−Nd anodes after 80 h polarization with constant current and pulse current

After the ohmic drop correction (Fig. 7), Tafel curves show two slopes. Their values were obtained by linear fitting separately at the low and high over-potential regions. The results are listed in Table 2. At the low over-potential region, the Tafel slope is about 114 mV/dec. For the PbO_2 electrode, when the Tafel coefficient b is near 120 mV/dec, the formation and adsorption of the OER intermediates is suggested to be the rate determination step [22]. However, at the high over-potential region, the Tafel slopes of pulse-current polarized anode increases to 158.8 mV/dec, about 10 mV/dec smaller than that of the constant current polarized Pb−Ag−Nd anode. The increase of Tafel slope may be related to the blocking effect of micro-pores by increasingly evolved O_2 at the higher over-potential region [23]. The smaller Tafel slope for pulse current polarized anode can be explained by a more intact anodic layer with fewer micro-pores, on which more O_2 bubbles are produced and evolved more easily. In industrial practice, the applied current density is 0.05 A/cm^2, which is located at the high over-potential region. Therefore,

Table 2 Oxygen evolution kinetics parameters of Pb−Ag−Nd anodes obtained from Tafel curves shown in Fig. 7

Current pattern	b_1/(mV·dec^{-1})	b_2/(mV·dec^{-1})
Constant current	114.1	168.7
Pulse current	114.7	158.8

the smaller Tafel slope at the high over-potential region could explain the lower anodic potential of Pb−Ag−Nd anode under pulse current polarization.

4 Conclusions

1) The anodic layer obtained through pulse current polarization is more intact and compact than that obtained through constant current polarization. In addition, the former has higher PbO_2 concentration, which could explain its lower anodic potential.

2) During the low current density period, the oxygen evolution is less intense, which benefits the recovery of porous anodic layer. Hence, the low current density period could be regarded as a ‘recovery period’.

3) The Pb−Ag−Nd anode under pulse current polarization presents smaller charge transfer resistance (R_{ct}) for OER and a smaller Tafel slope at the high over-potential region, which can further explain its lower anodic potential during pulse current polarization.

References

[1] CLANCY M, BETTLES C J, STUART A, BIRBILIS N. The influence of alloying elements on the electrochemistry of lead anodes for electrowinning of metals: A review [J]. Hydrometallurgy, 2013, 131−132: 144−157.

[2] MOHAMMADI M, ALFANTAZI A. Anodic behavior and corrosion resistance of the Pb-MnO_2 composite anodes for metal electrowinning [J]. Journal of the Electrochemical Society, 2013, 160(6): C253−C261.

[3] ZHANG Yong-chun, CHEN Bu-ming, YANG Hai-tao, GUO Zhong-cheng, XU Rui-dong. Anodic behavior and microstructure of Al/Pb−Ag anode during zinc electrowinning [J]. Transactions of Nonferrous Metals Society of China, 2014, 24: 893−899.

[4] ZHANG Wei, TU Chang-qing, CHEN Yi-feng, GEORGEOS H, XIAO Li. Effect of MnO_4^- and silver content on electrochemcial behaviour of Pb−Ag alloy anodes during potential decay periods [J]. Transactions of Nonferrous Metals Society of China, 2013, 23: 2174−2180.

[5] LARSON C, FARR J P G. Current research and potential application for pulsed current electrodeposition—A review [J]. Transactions of the IMF, 2013, 90(1): 20−29.

[6] WANG Jun-li, XU Rui-dong, ZHANG Yu-zhi. Influence of SiO_2 nano-particles on microstructures and properties of Ni−W−P/CeO_2−SiO_2 composites prepared by pulse electrodeposition [J]. Transaction of Nonferrous Metals Society of China, 2010, 20(5): 839−843.

[7] CHUNG C K, CHANG W T, LIAO M W, CHANG H C, LEE C T. Fabrication of enhanced anodic aluminum oxide performance at room temperatures using hybrid pulse anodization with effective cooling [J]. Electrochimica Acta, 2011, 56: 6489−6497.

[8] LEE W, SCHOLZ R, GÖSELE U. A continuous process for structurally well-defined Al_2O_3 nanotubes based on pulse anodization of aluminum [J]. Nano letters, 2008, 8(8): 2155−2160.

[9] XU R D, HUANG L P, ZHOU J F, ZHAN P, GUAN Y Y, KONG Y. Effects of tungsten carbide on electrochemical properties and microstructural features of Al/Pb−PANI−WC composite inert anodes used in zinc electrowinning [J]. Hydrometallurgy, 2012, 125−126: 8−15.

[10] TAGUCHI M, HIRASAWA T, WADA K. Corrosion behavior of Pb–Sn and Pb−2 mass% Sn−Sr alloys during repetitive current application [J]. Journal of Power Sources, 2006, 158(2): 1456−1462.

[11] MASSÉ N, PIRON D L. Effect of nickel in zinc electrowinning under periodical reverse current [J]. Journal of Applied Electrechemistry, 1990, 20: 630−634.

[12] LAI Y Q, LI Y, JIANG L X, LV X J, LI J, LIU Y X. Electrochemical performance of a Pb/Pb−MnO_2 composite anode in sulfuric acid solution containing Mn^{2+} [J]. Hydrometallurgy, 2012, 115−116: 64−70.

[13] CONWAY B E, LIU T. Characterization of electrocatalysis in the oxygen evolution reaction at platinum by evaluation of behavior of surface intermediate states at the oxide film [J]. Langmuir, 1990, 6(1): 268−276.

[14] LI W S, CHEN H Y, LONG X M, WU F H, WU Y M, YAN J H, ZHANG C R. Oxygen evolution reaction on lead−bismuth alloys in sulfuric acid solution [J]. Journal of Power Sources, 2006, 158(2): 902−907.

[15] YE Z G, MENG H M, SUN D B. New degradation mechanism of Ti/IrO_2 + MnO_2 anode for oxygen evolution in 0.5 M H_2SO_4 solution [J]. Electrochimica Acta, 2008, 53(18): 5639−5643.

[16] ZHONG Xiao-cong, GUI Jun-feng, YU Xiao-ying, LIU Fang-yang, JIANG Liang-xing, LAI Yan-qing, LI Jie, LIU Ye-xiang. Influence of alloying element Nd on the electrochemcial behavior of Pb−Ag anode in H_2SO_4 solution [J]. Acta Physico-Chimica Sinica, 2014, 30(3): 492−499.

[17] BISQUERT J, RANDRIAMAHAZAKA H, GARCIA-BELMONTE G. Inductive behaviour by charge-transfer and relaxation in solid-state electrochemistry [J]. Electrochimica Acta, 2005, 51(4): 627−640.

[18] FRANCO D V, SILVA L M D, JARDIM W F, BOODTS J F. Influence of the electrolyte composition on the kinetics of the oxygen evolution reaction and ozone production processes [J]. Journal of the Brazilian Chemical Society, 2006, 17(4): 746−757.

[19] BRUG G J, van den EEDEN A L G, SLUYTERS-REHBACH M, SLUYTERS J H. The analysis of electrode impedances complicated by the presence of a constant phase element [J]. Journal of Electroanalytical Chemistry and Interfacial Electrochemistry, 1984, 176(1−2): 275−295.

[20] YANG H T, GUO Z C, CHEN B M, LIU H R, ZHANG Y C, HUANG H, LI X L, FU R C, XU R D. Electrochemical behavior of rolled Pb−0.8%Ag anodes in an acidic zinc sulfate electrolyte solution containing Cl^- ions [J]. Hydrometallurgy, 2014, 147−148: 148−156.

[21] YANG H T, LIU H R, GUO Z C, CHEN B M, ZHANG Y C, HUANG H, LI X L, FU R C, XU R D. Electrochemcial behavior of rolled Pb−0.8%Ag anodes [J]. Hydrometallurgy, 2013, 140: 144−150.

[22] LAI Y, LI Y, JIANG L, XU W, LV X, LI J, LIU Y. Electrochemical behaviors of co-deposited Pb/Pb-MnO_2 composite anode in sulfuric acid solution — Tafel and EIS investigations [J]. Journal of Electroanalytical Chemistry, 2012, 671: 16−23.

[23] da SILVA L M, FRANCO D V, de FARIA L A, BOODTS J F. Surface, kinetics and electrocatalytic properties of Ti/(IrO_2+ Ta_2O_5) electrodes, prepared using controlled cooling rate, for ozone production [J]. Electrochimica Acta, 2004, 49(22−23): 3977−3988.

Pb−Ag−Nd 合金在 H_2SO_4 溶液脉冲电流极化过程中的电化学行为

钟晓聪[1]，于枭影[1]，蒋良兴[1]，李 飞[2]，李 劼[1]，刘业翔[1]

1. 中南大学 冶金与环境学院，长沙 410083；
2. 河南豫光锌业有限责任公司，济源 459000

摘 要：采用计时电位、SEM、XRD、EIS 和 Tafel 等方法对比研究 Pb−Ag−Nd 合金在 160 g/L H_2SO_4 溶液中的脉冲电流极化和恒电流极化过程中的氧化膜和析氧行为。研究结果表明：脉冲电流极化的 Pb−Ag−Nd 合金表面的氧化膜孔洞更少，膜层更致密。这是由于在脉冲电流极化过程中的低电流阶段析氧反应更缓和，有利于多孔氧化膜的修复，因此低电流阶段可作为氧化膜的“修复期”。Pb−Ag−Nd 阳极在脉冲电流极化过程中表现出更低的阳极电位，这与脉冲电流极化过程中阳极更小的传荷阻抗和高过电位区间更小的 Tafel 斜率相对应。更低的阳极电位可能与其氧化膜中更高的 PbO_2 含量有关，因为 PbO_2 可以促进析氧反应活性位点的生成。

关键词：铅基阳极；脉冲电流极化；析氧行为；氧化膜层

(Edited by Mu-lan QIN)